VYSOKÁ ŠKOLA
CHEMICKO-TECHNOLOGICKÁ
V PRAZE

Hydrogenolysis of dimethyl adipate over modified CuZnAl catalysts

Author: Jon Ander Garcia

Supervisor: Ing. David Kubička, Ph.D., MBA

Co-supervisors: Ing. Jaroslav Aubrecht

Ing. Viola Pospelova

Year: 2019

Department of Petroleum Technology and Alternative Fuels

CONTENT

INTRODUCTION

The purpose of this project is to perform stability tests of CuZnAl-based catalyst as a substitute to the copper-chromium Adkins catalyst used for ester hydrogenolysis reactions. This comes from the fact that chromium is a heavy and toxic metal and European Union have passed legislation to limit its industrial use. For this reason, this project has been framed inside green chemistry. CuZnAl was previously study as a substitute, but there is not enough data about the stability of the catalyst over long reaction periods of time that would be needed for industrial use. In this case, dimethyl adipate as a reactant was chosen and then hexane-1,6-diol as a product was detected.

In order to accomplish this purpose, several stability tests have been performed at different time intervals from 4h to 72h. These tests were performed in a fixed-bed reactor. The goal was to compare the effects of two different CuZnAl catalysts and different calcination temperatures on catalyst stability, performance and properties. Thus, parameters such as elemental composition, phase composition, specific surface area, particle and pore sizes etc. were measure. Meanwhile, the catalyst stability and performance were tested when the hydrogen pressure and temperature were kept constant at 100 bar and 205°C, respectively. Using this information, the influence of reaction time on catalyst activity and the influence of basic catalytic properties on the catalytic performance were analyzed.

LITERATURE REVIEW

This project can be framed within the branch of Green Chemistry, established in the 1990s, and defined as the design of chemical products and processes to reduce or eliminate the use and generation of hazardous substances[1]. This supposes a shift from the traditional concept of process efficiency that gives the value only to the highest chemical yield towards one assigning value of avoiding waste and the use of toxic substances[2]. For this purpose, we need to start from the design and conception of the process. If the design process is well planned, there is no need to have tradeoffs, but it may be possible to obtain synergies. To help with this, there are twelve principles of green chemistry that are needed to be considered.

They are as follows:

1. Prevention
2. Atom Economy
3. Less Hazardous Chemical Synthesis
4. Design Safer Chemicals
5. Safer Solvents and Auxiliaries
6. Designing for Energy Efficiency
7. Use of Renewable Feedstocks
8. Reduce Derivatives
9. Catalysis
10. Design for Degradation
11. Real-Time Analysis for Pollution Prevention
12. Inherently Safer Chemistry for Accident Prevention

As can be seen, they range from reducing the waste generated instead of having to treat it, using renewable feedstocks, or reducing the use of solvents or auxiliary substances whenever possible. As the topic has developed, it has become clearer that catalysis is a central part of green chemistry, because it can improve selectivity and therefore reduce unwanted products that will require treatment and cause a waste of energy and resources. Moreover, it can be important in the stability due to the deactivation of the catalyst, giving us a catalyst that doesn't need to be regenerated so often and thus, also reducing waste production. In our case, as stated, we focus on the catalyst toxicity topic.

These green chemistry principles can be applied to the hydrogenolysis of esters, which is a reaction between ester and hydrogen where hydrogen selectively splits a C-O bond adjacent to a carbonyl group. This reaction has been used for more than 50 years for the production of fatty alcohols from natural fatty acid esters[3], but can also be used to produce acids, hydrocarbons and ethers. Moreover, several processes have been proposed for the production of chemicals such as ethanol or methanol involving this the hydrogenolysis of an ester. In the same front, there has been continuous research in the last decades for substituting the energy-intensive production process of ethylene glycol and 1,4-butanediol for cheaper alternatives involving ester hydrogenolysis[4]. However, nowadays the hydrogenolysis of organic esters is performed using an Adkins catalyst. This catalyst is widely

used in industry and is formulated as $CuO.CuCr_2O_4$[5]. It is the preferred catalyst for the hydrogenation of esters to alcohols because of its capability to selectively hydrogenate carbonyl bonds while leaving unsaturated C=C virtually untouched[3]. However, since it contains chromium, which is a heavy metal, it possesses an environmental hazard. This is due to the waste that is created during the preparation of the Adkins catalysts[5], where the chromium solution used to produce the catalyst still contains chromium salts after catalyst preparation and thus has to be disposed of in a safe way. In a similar way, the catalyst has to follow a similar process when it reaches the end of its life cycle and becomes deactivated. The disposal rules for this element are very strict (the EPA and the EU heavily regulate its disposal and handling, since it is classified as heavy metal), so it does not meet the criteria for green chemistry, and thus substitute should be found[6]. When these Adkins catalysts are used for hydrogenolysis the reaction is performed under 25-35 MPa and temperatures from 250 °C to 350 °C[7]. So, from the economical point of view, it would be efficient to perform the reaction at better reaction conditions.

The copper is regarded to be the fundamental part of the hydrogenolysis process due to its low activity in the C-C bond hydrogenolysis and high activity for hydrogenolysis of C-O bonds. However, the copper properties (stability and activity) are not good enough[8] because of the sintering of its particles, whereas the particles are bonded together during the heating and it results in a surface area decrease. In case of our reaction, the sintering happens at a lower temperature than the reaction is carried out at[9]. Apart from particle sintering, carbon deposition, poisoning from raw materials, mechanical damage and leaching by the reaction can also lead to the destruction of the catalyst. This deactivation is highly related to the catalyst itself and the preparation process used to produce it, so modifying it can have a big impact on its performance. These characteristics can be improved by optimizing the experimental conditions, which directly affect the lifespan of the catalyst. This outcome can be achieved by optimizing the preparation method, which affects its internal characteristics or optimizing the application conditions of the catalyst, that affect its external activity. Another option is optimizing the supports used because they have a big influence on the morphology of the active phases, their interactions, the acidity and basicity, and the adsorption-desorption properties of reactant and product. By trying to confine the copper species into morphologically well-defined inorganic cavities, due to its different thermal and chemical stability compared to a conventional supported catalyst, improvements can also be achieved.[10] Finally, structural promoters can also be used, which consist in adding a second component to promote the activity and stability of the Cu catalyst. Among these promoters, Cr is used in the industrial catalyst today, because it modifies the stability of Cu, acts as an electron donor, helps it absorb hydrogen, increases dispersion and prevents sintering[11]. Then, there are new promoters being tested, such as Zn, which increases the dispersion of the Cu metal and thus giving us more active sites for the reaction to occur[12]; Al, that is credited with increasing the BET surface area, improving Cu dispersion and decreasing the sintering of the Cu particles at the temperatures we want to carry out our reaction[12]; Ag, restrains the aggregation of copper; Pd, where the charge transfer between Pd and Cu

increases the reducibility of the surface oxide; Ni, stabilizes the Cu species by insertion into the SiO_2 support[10]; and ruthenium or platinum additives on the copper lead to the disappearance of the adsorbed hydroxyl groups, thus eliminating the C-C and C-O bond cleavages. This is the result of the reduction of the hydroxylated copper induced by the hydrogen electrode potential composed of the hydrogen-ruthenium or hydrogen-platinum couple[13]. Based on the literature, we have focused on a mixture of Zn and Al as our structural promoters.

CuZnAl catalysts are nowadays mainly used for methanol production by hydrogenating CO_2 and CO mixtures at low pressures[12], but have also been used for hydrogen production by methanol reforming[14], hydrogen production from dimethyl ether[15], production of dimethyl carbonate from propylene carbonate with methanol and for the hydrogenation of esters to alcohols[11]. Lately, there have been some journal articles citing the use of this catalyst for the production of hexane-1,6-diol from dimethyl adipate[7], but no research has been done monitoring the stability of these catalysts.

HYDROGENOLYSIS OF DIMETHYL ADIPATE

In recent years, with the focus on the green economy and the concern over the sustainability of the manufactured goods, biodegradable polymers have been a hot topic. A lot of resources have been put into the production of this kind of polymers, with mixed results due to the physical properties of the polymers obtained. However, a polymer produced using 1,6-hexanediol, among other compounds, has been found to show good thermal, water absorption and hydrolytic degradation properties. For these reasons, we have focused our attention towards this compound[16].

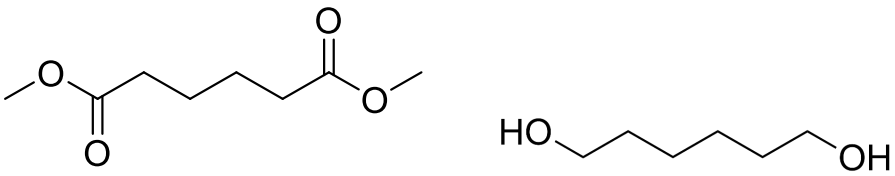

Figure 1: Chemical formula of dimethyl adipate (left) and hexane-1,6-diol (right)

Hexane-1,6-diol (HDOL) is currently used in the production processes of polyester and polyurethane, as a monomer for the production of polyesterpolyols, polycarbonate diols, acrylic monomers, diluents, adhesives and sealing compounds[17].

This HDOL can be obtained from dimethyl adipate, shown in Figure 1, by a hydrogenolysis reaction.

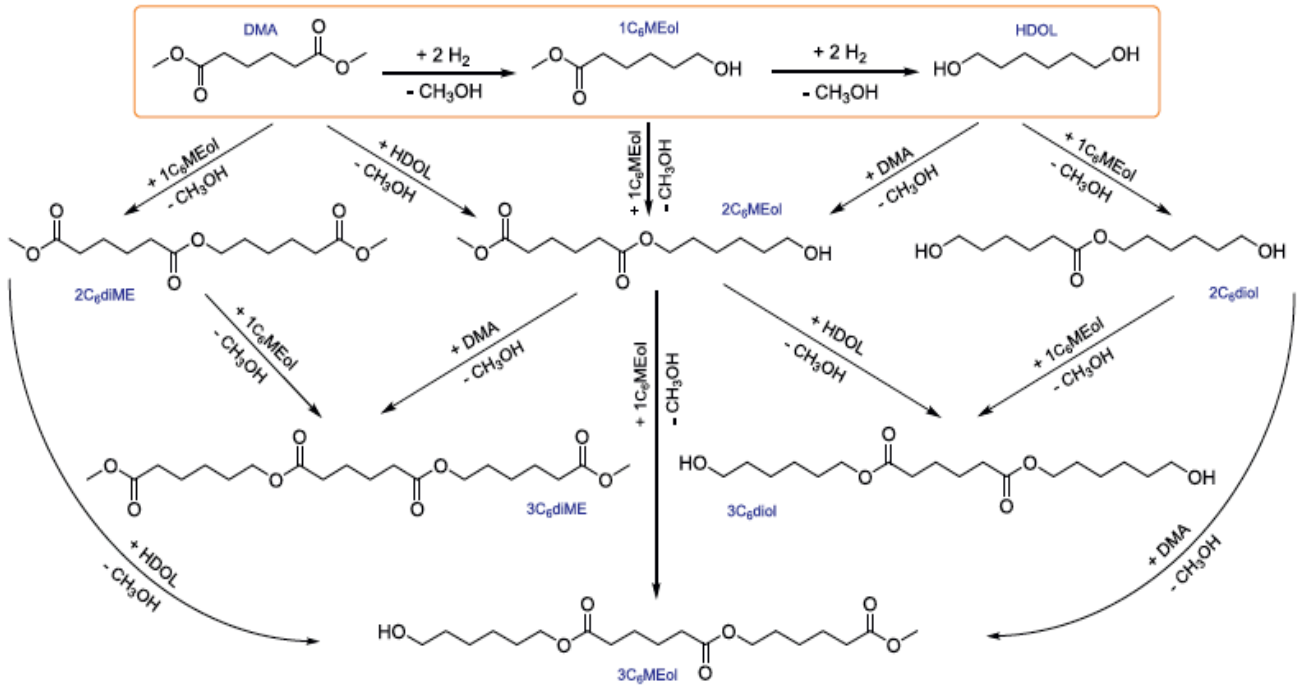

Figure 2: Proposed reaction network explaining the transesterification pathways during the hydrolysis of DMA[18]

However, as we can see in Figure 2, the reaction is not as straight forward as we might think, and a lot of unwanted products from the hydrogenolysis reaction should be expected, based on previous literature[18]. For example, two molecules can bond together instead of getting hydrolyzed. As can be seen, instead of getting hydrolyzed first to methyl-6-hydroxy hexanoate ($1C_6MEol$) and then to the desired HDOL, it can happen that any of them can merge to form new compounds as 6-methoxy-6-oxohexyl methyl adipate ,6-hydroxyhexyl methyl adipate or 6-hydroxyhexyl 6-hydroxyhexanoate($2C_6diME$, $2C_6MEol$ or $2C_6diol$ called in Figure 2 respectively) , or even 3 or more molecules fused together, but each subsequent one is less probable.

The range of products depends on the kind of catalyst used in the reaction. They can vary from methyl caproate and e- caprolactone if monometallic Ru was used[19], or adipic acid monomethyl ester, cyclopentanol, 2-methyl cyclopentanol and hexan-1-ol, when copper-based catalyst was used[18]. In the most promising case, where conversions over 90% were reached, methyl 6-hydroxyhexanoate was found mainly, indicating that it is an intermediate in the formation of HDOL. This intermediate appears when only one of the ester group is hydrogenated, leaving the one in the other side of the molecule intact, but making it possible to follow hydrogenation afterwards. When we analyze Figure 3, we can see other possible pathways the DMA molecule can follow when the hydrogenolysis is carried out.

It can also happen that a cyclic molecule is formed, and this is completely undesirable because it's not possible for it to react to form a HDOL molecule.

Another problem we can see is that if the residence time is too high, the HDOL that is formed can form 6-hydroxycaproic-6-hydroxyhexanelactone by transesterification of the HDOL molecule with MSH, or adipic acid-6-hydroxylhexyl-methyl ester by transesterification with DMA. HDOL can also cyclize becoming cyclopentanol, or suffer cyclization with some other reaction forming CPMOL, TMCOL or OP molecules (Figure 3). Apart from this, it can only lose an alcohol group forming 1-Hexanol.

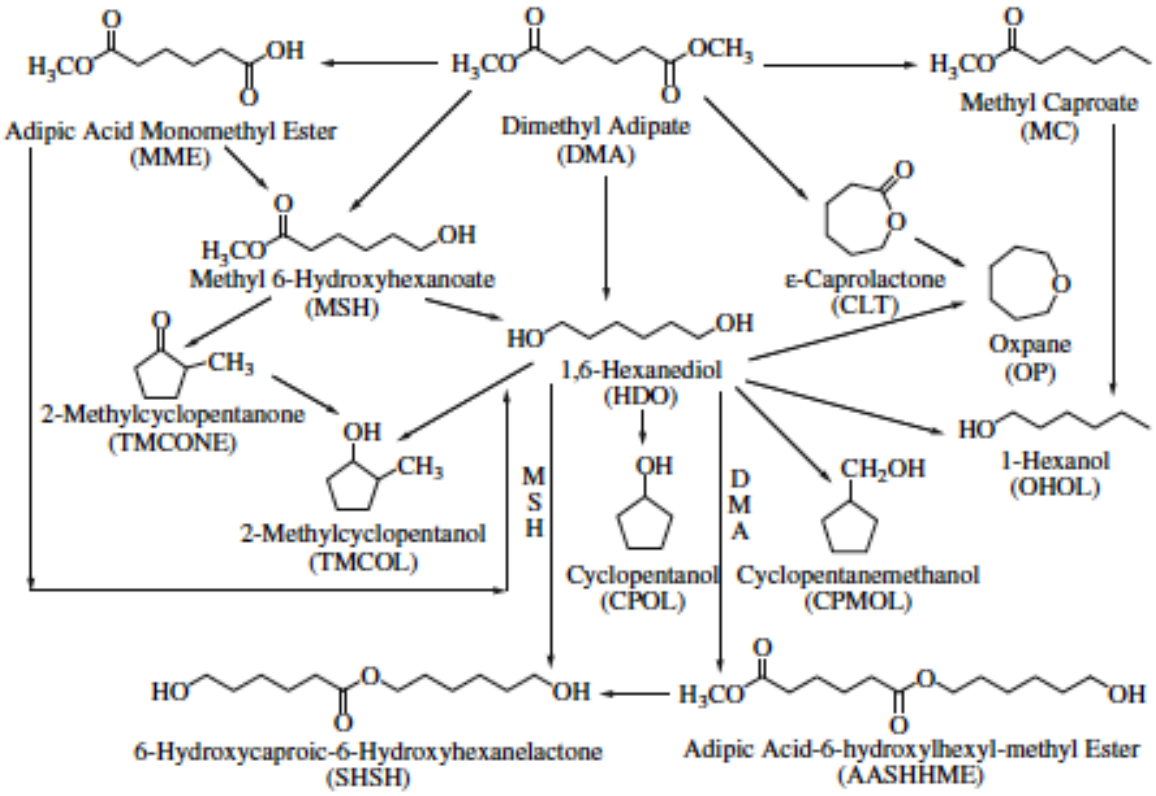

Figure 3: Simplified reaction scheme for hydrogenation of dimethyl adipate[7]

In recent years, there have been efforts made trying to find alternative catalysts, mainly based on noble metals, but no great success has been achieved, and modifications have to be made, such as combining them to form bimetallic compounds or using special preparation methods to improve the selectivity and conversion[20].

In order to avoid some of these undesired reaction pathways, some different bimetallic catalysts have been tested with the intent to substitute the chromium in the Adkins catalyst, as stated before. Some examples of these catalysts are $RuSn/TiO_2$[19]; Pt/Al_2O_3 [21]; $RuSn/Al_2O_3$[7] and $RuSn/TiO_2$[22], which have been tested in the hydrogenation of DMA. Also, copper-based catalysts have been found useful in the hydrogenation of carbon-oxygen bonds, such as Cu/SiO_2[23], when optimizing the experimental conditions CuZnAl-773[24] was among the better performing. Cu-Co/HMS[25], $Cu\text{-}Ni(2)/SiO_2$ or $Cu\text{-}0.5\%Pd/SiO_2$[26] were found among the candidates when the approach is to use a structural promoter to improve the properties of

the catalyst and Cu/Al-ZrO_2 showed good results when trying to design from confinement effect. The strategy was to optimize the supports when using Cu/ZrO_2[4] and Cu/SiO_2-TiO_2[27]. When looking at previous experiments, most of the tests were carried out at temperature under 215 °C and 5 MPa, showing promising results[7], but a short summary of every condition used in the test can be found in a mini review[10].

CuZnAl catalyst synthesis and properties

If we look at literature of recent research on the CuZnAl catalyst when used for hydrogenation of esters to alcohols, there are some methods of preparation that can be used, depending on what is the goal. Methods of catalyst preparation are very diverse and a catalyst may be prepared via different routes, but all can be summarized in three basic steps: preparation of the primary solid associating the useful components, processing of the primary solid to obtain the catalyst precursor, and the activation of the precursor to give the active catalyst[28]. In the first step, there are several methods, but the most used ones are impregnation, precipitation and co-precipitation, gel formation, physical/direct mixing method, and some other minor methods, but the major ones are the two first ones.

Impregnation consists in contacting a solid with a liquid containing the components to be deposited on the surface. Within the method, there are several subtypes, depending on the properties looked for, like impregnation by percolation, co-impregnation, successive impregnation, etc. The advantages of catalysts prepared with this method are their high surface-to-volume ratio and the high thermal stability endowed by the dispersion[28].

The other major method, co-precipitation, consists of a phase association of one or several elements. The method can be divided into two steps: nucleation and growth, where one is performed far from equilibrium, exceeding the solubility constant; and the other in which the conditions slowly go towards equilibrium. This method presents a major advantage, in that a large number of nanoparticles can be synthesized in a short time. However, it does not in general produce homogeneous precipitates, and a precipitation agent is needed in the process. Since the catalyst for the project consists of copper, aluminum and zinc, this will be the appropriate method for the preparation, since three phases are needed to be associated.

In this case, copper, zinc and aluminum nitrates [$Cu(NO_3)_2{\cdot}3H_2O$, $Zn(NO_3)_2{\cdot}6H_2O$ and $Al(NO_3)_3{\cdot}9H_2O$)][7,11] will be used as Cu, Zn and Al precursors. However, $Cu_2(OH)_2CO_3$, ZnO and $Na_2Al_2O_4{\cdot}3H_2O$, with an appropriate amount of formic acid have also been used in other cases[29], and yielded the same concentrations and compositions as when using nitrates. Na_2CO_3 or NaOH[30] are common precipitation agents used in the preparation of this catalyst. These separate aqueous mixtures are then mixed at pH in a range of 6.5-9 and left for ageing. Final procedures are filtering, washing and drying. The following step is the treatment to obtain the precursor. This step can include the drying, thermal decomposition of the salts, calcination, and much more. In this particular case, after drying, the catalyst is to be calcined

in air atmosphere at temperatures ranging from 330 to 600[7,29] for a time between 3 and 5h[7,29,30].

To characterize the obtained results, from both the precursor and the calcined catalyst, the XRD analysis was performed on the samples. This technique is the most suitable for the identification of the crystalline phases present in the catalyst but is also used to identify the particle sizes of these crystallites.

Using this technique, it can be seen that the main phase crystal phase in the industrially produced CuZn-based catalyst is zincian malachite[31]. However, using different precursors, different calcining conditions and different precipitating agents, different crystalline phases could be produced.

In previous literature, it can be seen that Hydrotalcite like compounds such as $[Zn_{0.64}Al_{0.36}(OH)_2(CO3)_{0.18}\cdot 0.86H_2O]$[14], $Cu_3Zn_3Al_2(OH)_{16}CO_3\cdot 4H_2O$ and $(CuZn)_2Al_2(OH)_{16}CO_3\cdot 4H_2O$ are present in the as-prepared catalyst. We can also find malachite $[Cu_2CO_3(OH)_2]$, aurichalcite $[Cu_2Zn_3(CO_3)_2(OH)_6],)$[32] and zincian Malachite $[(Cu_{0.8}Zn_{0.2})_2(OH)_2(CO_3)]$[33] in case of different preparation methods.

Depending on the phases present on the catalyst, the activity will be different. For example, zincian malachite is the major phase of industrial CuZnAl catalyst when used for methanol production, and on the contrary, hydrotalcite is regarded as an undesired precursor due to encapsulating the active Cu particles[33].

Also, when the Al concentration was higher than 6.5%, the zincian malachite phase content decreased[33].

The pH of the solution when preparing the catalyst affects the crystal size of Cu, the higher the pH, the smaller the Cu crystallite size, which affects the selectivity to some products; but also have little effect on the crystalline phases of the samples[33].It has also being noted that the preferred crystalline phase for methanol synthesis reaction is aurichalcite, and it appears with a more acidic pH preparation process[34].

Also, the precipitation agent can have an effect. The mixture of NaOH and Na_2CO_3 instead of pure Na_2CO_3 helps prevent the formation of carbon richer phases such as malachite[33].

In addition, the temperature of subsequent calcination step affects the phase composition of calcined catalyst. In respect to this variable, the higher it is, the larger crystallites will be in the catalyst, and subsequently, lower activity will give the catalyst due to smaller surface area etc.[34]

Finally, the catalyst needs to be activated, and the activation process is the catalyst reduction by hydrogen. Common temperature used for the reduction is around 300 °C .

EXPERIMENTAL PART

MATERIALS

Table1. List of used chemicals

Name	Supplier	Purity
Acetone	Penta	>99%
Dimethyl Adipate	Merck KGaA	>99%
Butanol	Penta	>99.5%
Ethanol *for washing*	BIOFERM	95%
Hydrogen	SIAD	99.9%
Nitrogen	SIAD	99.999%

CATALYST PREPARATION

Two catalysts were prepared by the co-precipitation method in a University research center. The obtained as-prepared catalysts were calcined in a muffle furnace in air atmosphere for 3 hours at 350 °C or 550 °C with a heating ramp of 2 °C per minute.

After the calcination the particle size distribution was modified to get a particle size between 0.1 and 0.25 mm. In order to achieve this, first, the calcined catalyst had to be tableted. Then the catalyst was grinded to smaller particle sizes, and finally these particles were classified in the desired particle sized needed for the experiment (0.1-0.25 mm).

INSTRUMENT DESCRIPTION

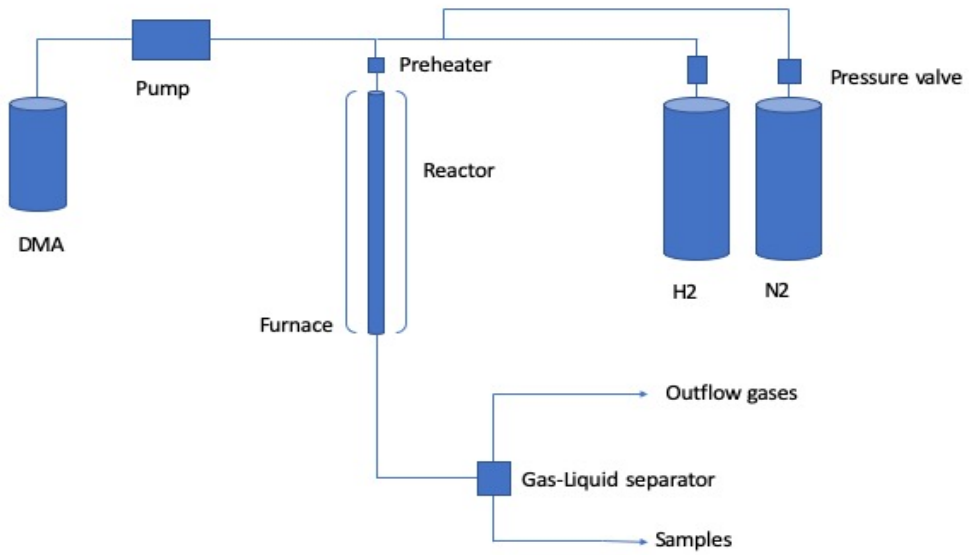

Figure 6. Basic scheme of the reactor

The basic scheme of the apparatus used for the performing of the experiments is seen in Figure 6. First, the pump makes the inlet chemical flow to the reactor simultaneously with gases. The unit is also equipped with a preheater. After this, the mixed stream goes through the reactor that is surrounded by a computer-controlled heating coat that keeps the reactor at the desired temperature. The gas-liquid products are separated in a (g)-(l) separator and liquid samples are collected from the tube after valves.

CATALYTIC TESTING

The reactor was loaded with 4 g of the calcined catalyst in the middle section, filling the rest of the reactor capacity with silicon carbide and adjusting its quantity inverse proportionally to the amount of catalyst used to have totally 11 ml. At both ends of the reactor, a silica wool filter must be placed in order to prevent the catalyst and the carbide from flowing out when the reactor is pressurized.

Then a pressure test was performed to ensure pressure would be held for all the duration of the experiment. The procedure was performed as follows. First, all the valves were closed. Then, the three-way outlet valve, directing the outlet gases directly to the atmosphere or through a flowmeter, was put in the atmosphere position. With this done, now the pressure was increased using the bypass valve from the hydrogen bottle. Two steps were followed: first, a slow increase to 50 bar, and then to 100 bar, checking at both instances the absence of any leakage by the use of soapy water or a leak detection fluid. This is critical, because since the reactor has a lot of joining points, a lot of weak spots where leaks can happen exist and every weak spot must be checked prior to starting the reaction.

When it was sure that no leaks were present, the pressure was released by opening the outlet valve, and after that, the electronic outlet valve was slowly opened by the computer control. Once all the hydrogen pressure was released, the nitrogen source was set, opening the nitrogen bottle and setting the pressure to 8 bar, and all the thermocouples were connected to data logger.

Before the experiment, the catalyst was reduced *in situ*. The reduction was performed at 220°C under a nitrogen/hydrogen atmosphere. Since the reduction is a very exothermic process, the hydrogen concentration had to be slowly increased. First, only nitrogen was flowing with a flow rate of 30 $l.h^{-1}$ and then the hydrogen concentration was slowly increased. The procedure was following: hydrogen flow rate was increased by increasing 0.1 $l.h^{-1}$ every minute from 0 till 2 $l.h^{-1}$, then it was kept for 10 minutes, and then the nitrogen flow was decreased until it was stopped, decreasing with 10% every 3 minutes. Due to the unwanted temperature increase, the temperature of the reactor was continuously monitored during the reduction reaction. When the temperature started to decrease signaling that the reduction was completed, the outlet valve was set to hold 100 bar pressure.

CATALYTIC TESTING

The reduced catalyst was used for the experiment. The hydrogen pressure was 100 bar, the hydrogen flow rate was set to 16 $l.h^{-1}$, and the reaction temperature was set to 205 °C using the heating performance of the furnace. While the furnace heated up, the DMA flow rate was 16 $l.h^{-1}$. Now, the temperature was monitored through the computer and samples were taken every two hours for different periods of 4, 12, 24, 48 and 72 hours.

After the experiment, the furnace was set off and opened, to help cooling down the reactor, and the DMA flow stopped. When the reactor temperature reached below 60°C, ethanol was fed into the reactor with a flow rate of 3 $ml.min^{-1}$. It was kept for 10 minutes with the ethanol flowing, and after that the pump was set off, hydrogen was kept flowing until ethanol stopped coming out to the outflow deposit.

Finally, after washing of the catalyst, the reactor was disassembled, and the catalyst unloaded. The silicon carbide was disposed of, while the catalyst was stored. As the last step, the reactor was cleaned by using a solvent, ethanol or acetone, and pressured air.

PRODUCT ANALYSIS

Samples taken during the experiments were prepared for GC analysis. The samples (two droplets ca. 20 µl) were prepared by diluting 20 µl of the sample (ca. two droplets) and with 1.5 ml of butanol. Then, the mixture was injected for analysis using a gas chromatography machine model Hewlett Packard 5890. For analyzing the products obtained in the reaction, first of all, the possible products were identified and their residence times in the GC was determined. The following residence time (table 2) were obtained for the most probable products.

Table 2. Compounds residence times

Abbreviation	Full name	Residence time, min
HDOL	hexane-1,6-diol	11.1
$1C_6$MEol	methyl-6-hydroxy hexanoate	12.1
DMA	1,6-dimethyl adipate	13.1
$2C_6$diME	6-methoxy-6-oxohexyl methyl adipate	23.9
$2C_6$MEol	6-hydroxyhexyl methyl adipate	24.4
$2C_6$diol	6-hydroxyhexyl 6-hydroxyhexanoate	24.9
$3C_6$diME	bis(6-methoxy-6-oxohexyl) adipate	32.8
$3C_6$MEol	6-hydroxyhexyl (6-methoxy-6-oxohexyl) adipate	33.1
$3C_6$diol	bis(6-hydroxyhexyl) adipate	33.4

With this data and the areas given by each product in the GC, the conversion and selectivity were calculated by integrating the area under the peaks at the mentioned retention times. To convert these areas to a molar percentage, with which the selectivity and conversion of

each test could be calculated, the response factor and the molecular weight of each compound was used. The response factor is defined as the ratio between a given concentration of a compound and the response given by the detector, *i.e.*the area detected under a peak. These factors were obtained during the calibration process of the GC. Finally, the conversion and selectivity obtained at each test was calculated by means of the following definitions (Equation 1 and 2).

Conversion of DMA was calculated as the number of DMA moles over the initial moles.

$$Conversion = \frac{Number\ of\ DMA\ moles\ in\ the\ end}{Number\ of\ DMA\ moles\ in\ the\ beggining\ of\ the\ reaction} \quad (1)$$

Similarly, the selectivity towards HDOL was calculated as follows.

$$Selectivity = \frac{Number\ of\ HDOL\ moles}{Number\ of\ 1C_6, 2C_6\ and\ 3C_6 moles} \quad (2)$$

CATALYST CHARACTERIZATION

AAS was used to determine elemental composition using Agilent 280FS AA, where a mixture of acetylene and air was used as an atomization flame

XRD was used to determine phase composition of the catalyst using a diffractometer PAN analytical X'Pert3 Power and Cu Kα radiation. The XRD patterns were recorded in a range of 2θ = 5° - 70°. The crystallite sizes were calculated using the Scherrer's equitation

Apart from this, it is also used to identify the particle sizes of these crystallites, using the Scherrer equation.

$$\tau = \frac{K\,\lambda}{\beta \cos\theta}$$

Where τ is the mean size of the ordered (crystalline) domains, which may be equal or greater to the grain size, K is a dimensionless shape factor, with a value close to unity, λ is the X-ray wavelength, β is the line broadening at half the maximum intensity in radians and θ is the Bragg angle. Reflections at 2θ = 31.7° and 38.6° were used for the crystallite size calculations for ZnO and CuO respectively.

Equilibrium adsorption isotherms of nitrogen were measured at 77 K for calcined and spent catalysts using a static volumetric adsorption system (TriFlex analyzer, Micromeritics, Norcross, USA). The samples were degassed at 473 K (12 hours) prior to N2 adsorption analysis, in order to obtain a clean surface. The adsorption isotherms were fitted using the

Brunauer-Emmett-Teller (BET) method for the specific surface area [28] and the BJH method for distribution of mesopores.

A TPR analysis was performed to acquire knowledge about the appropriate reduction temperature to procced the tests. In this process, a mixture of argon and hydrogen were used, at a flow rate of 50 ml per minute, and a heating ramp of 5°C per minute with a target temperature of 1000°Cusing a machine model Quantachrome ChemStar TPx instrument with a TCD detector.

EXPERIMENTAL RESULTS

In this work, two prepared catalysts were characterized and then tested in dimethyl adipate hydrogenolysis for different time-on-stream to observe the catalyst stability.

CATALYST CHARACTERIZATION

1. AAS analysis

The mass and atomic composition of the as-prepared catalysts were obtained by means of AAS analysis. Results are seen in Table 3 and 4. The results showed that the catalysts had similar Al content and the difference is in Cu/Zn ratio. The copper to zinc ratio was 2.0 in the first catalyst (K18), while 1.5 in the latter (K19). Nonetheless, the aluminium to the sum of copper and zinc ratio was very similar in both cases, around 0.1 (Table 5). There is no need to use this analysis for the analysis of catalysts in the further stages because the atomic and molecular composition of the metals do not change when the catalyst is calcined or spent.

Table 3. Mass composition

Sample	Cu (wt.%)	Zn (wt.%)	Al (wt.%)
K18_prep	62.9	33.2	3.9
K19_prep	56.9	39.6	3.5

Table 4. Atomic composition

Sample	Cu (at.%)	Zn (at.%)	Al (at.%)
K18_prep	60.3	30.9	8.8
K19_prep	54.9	37.1	8

Table 5. Atomic ratios

Sample	Cu/Zn	Al/(Cu+Zn)
K18_prep	2	0.09
K19_prep	1.5	0.08

2. XRD analysis

2.1 As-prepared catalyst

Looking at the crystalline phases present in the as-prepared catalysts, it is noticeable that the main crystalline phase is zincian malachite in both of the catalysts. According to the previous literature, it is the phase commonly present in commercial CuZnAl catalysts used mainly for methanol production[33], however, we cannot confirm it is beneficial for DMA hydrogenolysis. Next to the zincian malachite, Aurichalcite was also detected in both samples, with a small

hydrotalcite signal in the K19 catalyst sample. In the as-prepared catalysts, we can detect the aluminium-containing phase due to the fact that hydrotalcite is crystalline.

Table 6. Crystalline phases present in as prepared catalyst

Sample	Zincian Malachite $(Cu_{0.8}Zn_{0.2})_2\ (OH)_2\ (CO_3)$	Aurichalcite $Cu_2Zn_3(CO_3)_2\ (OH)_6$	Hydrotalcite $(Zn_{0.66}Al_{0.34})OH_2(CO_3)_{0.17}\ (H_2O)_{0.7}$
K18_prep	Very strong	Weak	Not detected
K19_prep	0.86	0.09	0.05

2.2 Calcined catalyst

Looking at the calcined catalyst, we see in Table 7 that the major phase is tenorite CuO. However, we can also see the zincite present in the catalyst that based on the literature review, affects the behaviour of copper, by increasing its dispersion[12]. When the catalyst is calcined, the present hydroxycarbonates are decomposed, giving also gahnite, that is partially crystalline and detectable by XRD (Table 8). Nonetheless, the major part of aluminum created could be in the amorphous phase generally written as a $(Cu,Zn)Al_XO_Y(CO_3)_Z$, which is non-detectable by XRD.

Table 7. Crystalline phases present in calcined catalyst

Sample	Zincite(ZnO)(%)	Tenorite(CuO)(%)	Gahnite(ZnAl2O4)(%)
K18_350	ND	100	ND
K19_350	12	76	12
K19_550	25	75	ND

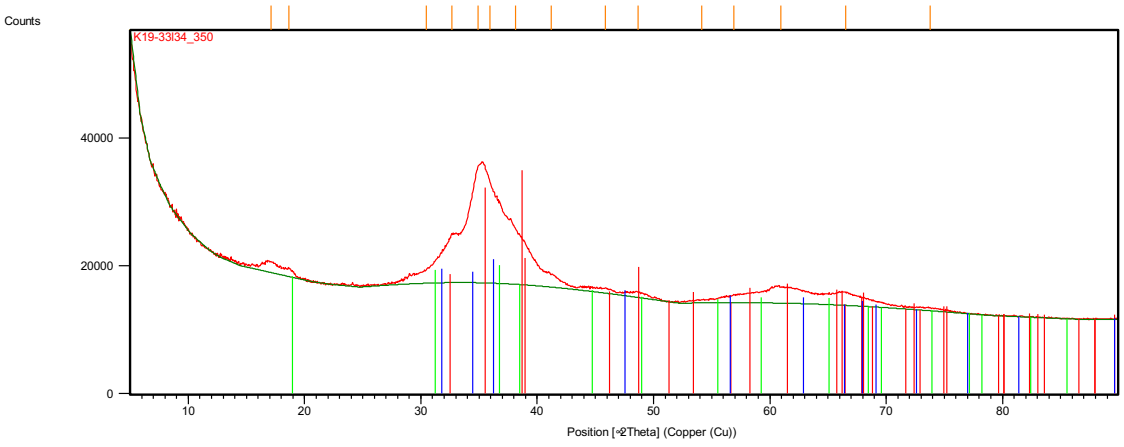

Figure 7. XRD pattern of K19_350

In Figure 7 and 8 the XRD patterns of the k19 catalyst calcined at 350 and 550C are shown. The figures should be used as a visual help for understanding the samples, not as quantitative data, since crystalline phase data is in the previous table. From the graph, it can be seen that the higher temperature sample is more crystalline, has more define peaks, and thus, probably the data obtained will be more accurate.

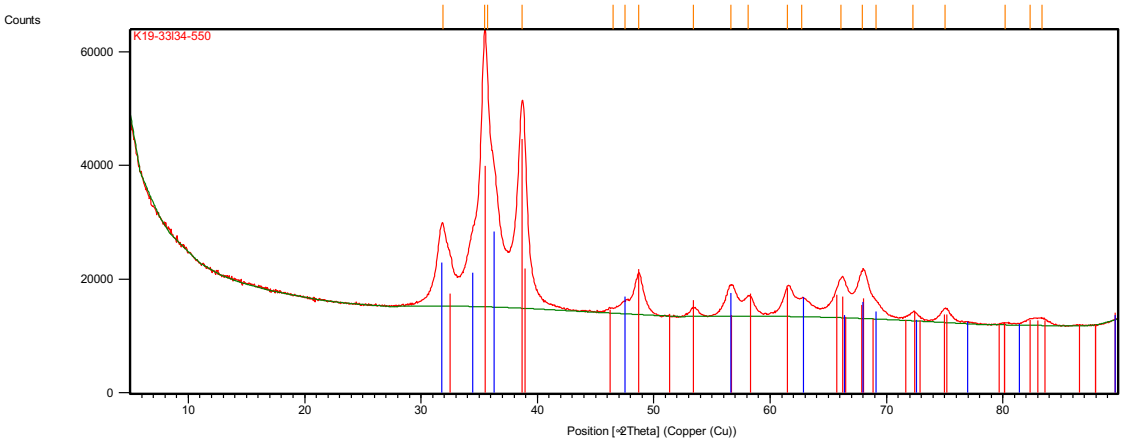

Figure 8. XRD pattern of K19_550 catalyst

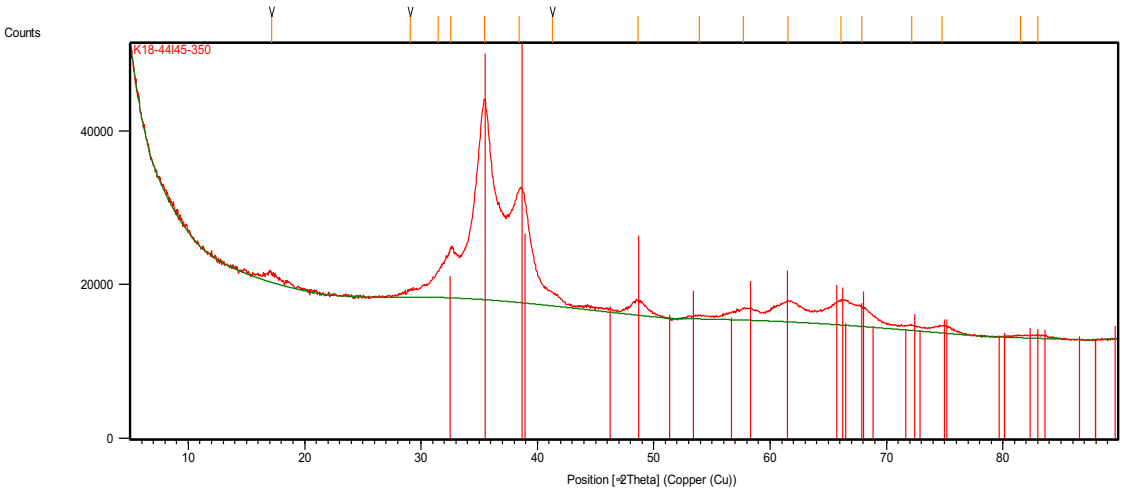

Figure 9. XRD pattern of K18 catalyst

Also, in Figure 9 the XRD results of the K18 catalyst are plotted. Here, a lot of signals are detected, and the peaks are very sharp, indicating non-amorphous phases are present. However, all the peaks are related to CuO, as identified in Table 7.

When comparing the crystallite sizes, it can be seen in Table 8 that at the higher calcination temperature, the sizes are bigger. Also, it can be seen that in the case of 350 calcination temperature, the K18 gets higher sizes than the k19. This is an undesirable effect, since with higher crystallite sizes, the available surface area is smaller, as will be seen in table 12. This

is a sign that the performance will be lower, as stated in the previous literature[7], but it will be seen in the results from the catalytic tests.

Table 8. Crystallite sizes in calcined catalysts

Sample	Zincite(ZnO)(Å)(31.7°)	Tenorite(CuO)(Å)(38.6°)
K18_350	ND	34.4
K19_350	31.6	21.5
K19_550	58.8	82.8

2.3 Spent catalyst

In Table 9 can be observed the change in the phase composition of spent catalysts when the catalytic experiments were performed. The catalyst used in experiments 1 to 4 corresponds to the K18 catalyst while 5 to 7 to K19. All spent catalysts have ZnO and Cu(0) as major phases that confirm that reaction was performed over metallic copper [Cu(0)]. SiC present in the sample came from small contamination during the unloading of the catalyst, because the inert silicon carbide was used as a filler in the reactor. Some catalysts contained CuO and Cu_2O that could be formed by the oxidation during the exposure of the catalyst to the air atmosphere during the unloading of the reactor. It was observed in all the samples to a smaller or greater extent.

Table 9. Crystalline phases present in spent catalysts

Sample	ZnO	Cu	SiC	CuO	Cu_2O
CuZnAl_1	40	43	17		
CuZnAl_2	38	42	20		
CuZnAl_3	31	15		37	17
CuZnAl_4	23	44	33		
CuZnAl_5	35	6		42	17
CuZnAl_6	32	8		39	20
CuZnAl_7	46	45			

Table 10. Reaction conditions of each experiment

Sample	Test duration, h	Temperature, °C	Pressure, bar	Catalyst
CuZnAl_1	4	205	100	K18-350
CuZnAl_2	48	205	100	K18-350
CuZnAl_3	24	205	100	K18-350
CuZnAl_4	72	205	100	K18-350

CuZnAl_5	24	205	100	K19-350
CuZnAl_6	12	205	100	K19-350
CuZnAl_7	14	205	100	K19-550
CuZnAl_8	5	205	100	K19-550

When observing the size of the crystallites showed in table 10, some kind of stability can be seen. The ZnO crystallites are in range of 45-70 Å while the copper oxide crystallites are between 69-75 Å. If CuO sizes are compared with the calcined catalyst, where the CuO size is 34 Å for the catalyst used in experiments 1-4 and 21.5 Å in experiments 5-6, it is noticeable that copper has undergone some kind of sintering or agglomeration. Finally, in the case of metallic copper, there seems to be a high variance in the particle sizes, getting from 60 Å up to 102 Å with one exception in fourth experiment.

Table 11. Crystallite sizes obtained by XRD

Sample	ZnO (Å)	CuO (Å)	Cu (Å)
CuZnAl_1	70		102
CuZnAl_2	46		80
CuZnAl_3	49	75	75
CuZnAl_4	66		160
CuZnAl_5	59	75	61
CuZnAl_6	52	69	82
CuZnAl_7	73		102
CuZnAl_8			

3. BET analysis

BET analysis was performed on the calcined and spent catalysts. Comparing the calcination temperatures (350 and 550 °C) of the K19 catalyst, the surface area decreased by 50%, from 104 to 57 $m^2.g^{-1}$, volume of the pores decreased by 60%, from 0.663 to 0.26 cm^3g^{-1}, and their average diameter went from 23.9 to 16.9 nm for the 550°C calcined sample, hinting a better performance in the reaction. This was expected, since in previous literature, at higher calcination temperatures, the CuO particles started to agglomerate, giving bigger particles with smaller pore sizes[7]. In the previous article[7], the optimum temperature appeared to be at 500 °C, with the agglomeration starting at 600 °C. However, it was observed that at 550 °C, the agglomeration is already noticeable and harms the performance of the catalyst.

Also, comparing the K19 and K18 catalysts calcined at 350 °C, the K19 BET surface area 20% better for K19, being 83 $m^2.g^{-1}$ in K18 while 104 $m^2.g^{-1}$ in K19, where the Cu/Zn ratio was 1.5, compared to 2 in K18, indicating that a higher concentration of zinc provides better structural properties . The pore diameters were practically equal. This does not necessarily correlate to

a 20% improvement in the catalytic performance, as will be seen in the catalytic test discussion.

During the experiment, catalysts properties are changing. The drop happened in the BET surface area, coming down from 83-104 $m^2.g^{-1}$ to 64-82 $m^2.g^{-1}$ during the all experiments, as well as the volume of the pores, going from 0.51-0.63 cm^3g^{-1} to 21-31 cm^3g^{-1}. However, in the case of K19 catalyst calcined at 550 °C, there does not seem to be any decrease in the BET surface area or in the volume of the pores.

Table 12. Results gained from nitrogen physisorption

Sample	BET surface area, $m^2.g^{-1}$	Volume of pores, cm^3g^{-1}	Average pore diameter, nm
K18-350	83	0.51	24.6
CuZnAl_1 (K18-350)	47	0.21	16. 6
CuZnAl_2 (K18-350)	75	0.29	13.9
CuZnAl_3 (K18-350)	64	0.27	15.4
CuZnAl_4 (K18-350)	70	0.23	12.3
K19-350	104	0.63	23.9
K19-550	57	0.26	16.9
CuZnAl_5 (K19-350)	78	0.31	14.1
CuZnAl_6 (K19-350)	82	0.31	13.4
CuZnAl_7 (K19-550)	64	0.31	17.4
CuZnAl_8 (K19-350)	77	0.26	12.2

4. TPR analysis

Finally, a TPR analysis was performed to determine the most appropriate temperature at which to perform the reduction of the catalyst prior to having the activity test done.

The result of this test can be seen in Figure 10, where the detector signal is plotted against the temperature. Looking at Figure 10 two major peaks can be seen, one at around 220 °C, and a smaller one at around 450 °C. With these peaks it can be deduced that most of the copper is reduced at this two temperatures, the most of it happening at 220 °C. Most probably, at 220 °C, the copper present in the surface is reduced, while at the higher temperature, the one in the inner layers or the structure gets reduced. With this information, the reduction temperature for the test was set up at 220 °C. Another probable reason for the existence of the secondary peak is that hydroxycarbonates present in the catalyst were decomposed at this higher temperature.

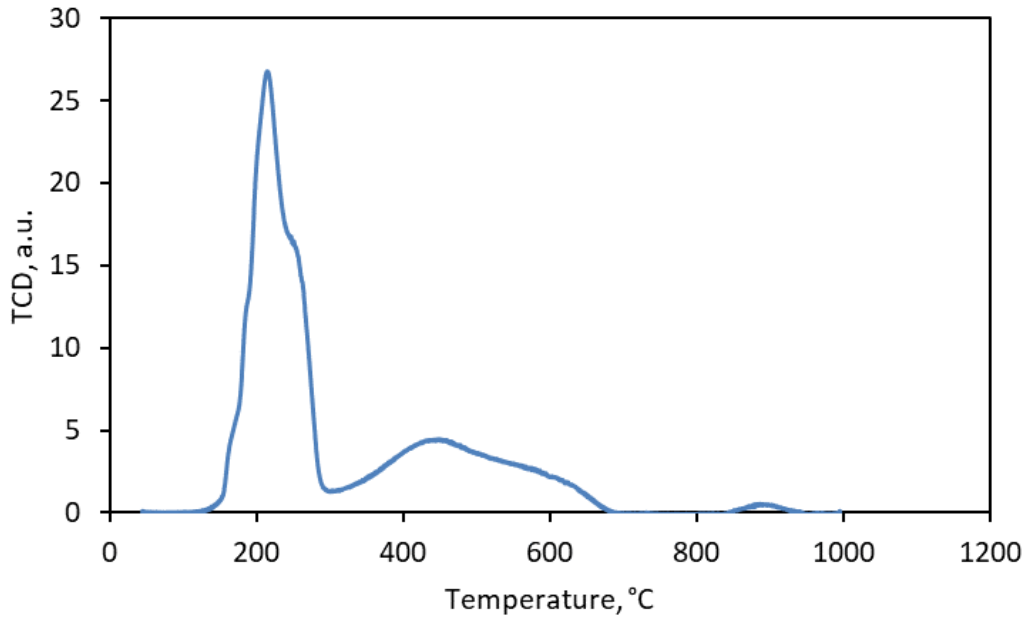

Figure 10. TPR temperature chart

The theoretical value of hydrogen consumption was calculated by taking into account the copper concentration in the catalyst. By seeing this results several conclusions can be inferred. First of all, the calcined catalyst consumed more hydrogen due to the fact that it had more oxidized phase CuO than the spent one. Moreover, the spike seen in experiment 3 can be explained for the higher concentration of CuO given by the XRD analysis. This is probably, as stated before, for the rapid oxidation during the unloading of the reactor. After, we see that the real hydrogen consumption by the calcined catalysts is lower than the theoretical one. That confirmed the presence of metallic copper but still some CuO must be present. The most probable reason for that is the fact that the Cu^{2+} ion is embedded within the amorphous Zn-Al oxide matrix, not allowing a total reduction to metallic copper. This is linked to the presence of hydrotalcite phase[33].

Table13. TPR Results

Sample	H_2 consumption	H_2 theoretical consumption	Real/Theoretical
K18-350	131	178	73%
CuZnAl_1	30		
CuZnAl_2	31		
CuZnAl_3	69		
CuZnAl_4	36		
K19-350	123	161	76%
CuZnAl_5	131		
CuZnAl_6	64		
K19-550	78	161	81%
CuZnAl_7	21		
CuZnAl_8	51		

Now, we can try to see a correlation between the activity, or reducibility of the catalyst, with the BET surface area and the Cu pore sizes, to see if there is a correlation. This is shown in Table 14.

Table 14. BET, particle size and reducibility comparison

Sample	H2 consumption	BET surface area, $m^2.g^{-1}$	Cu (Å)
CuZnAl_1	30	47	102
CuZnAl_2	31	75	80
CuZnAl_3	69	64	75
CuZnAl_4	36	70	160
CuZnAl_5	131	78	61
CuZnAl_6	64	82	82
CuZnAl_7	21	64	102
CuZnAl_8	51	77	

It is very clear that the reducibility of the catalyst is inversely related to the size of the copper particles in the catalyst. With the highest copper particle sizes, the hydrogen consumption was the lowest, signalling that copper molecules were encapsulated, as stated before, and efforts should be made to keep this size the lowest possible.

CATALYTIC DATA

In this thesis, we tested two types of catalysts as stated above, K18 and K19. Catalytic tests of different time-on-stream were performed, from 4 to 72 hours, but all of them at the same temperature of 205ºC and hydrogen pressure of 100 bar. Tested catalysts were calcined at different calcination temperatures but reduced at the same temperature of 220ºC.

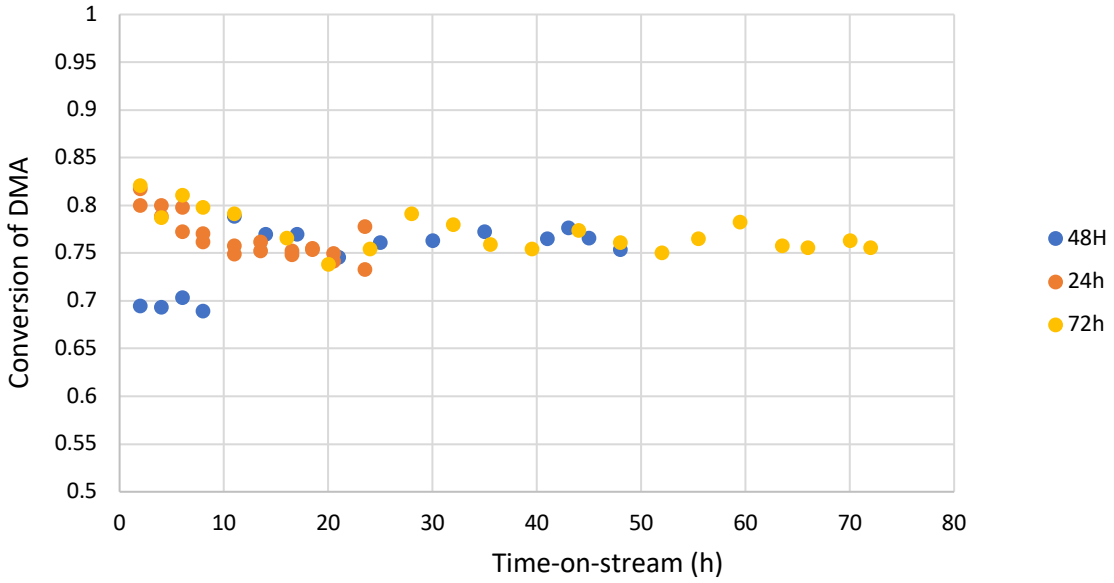

Figure 11. Conversion of DMA over K18 catalyst

In Figure 11, we can observe the tests performed with the catalyst K18 that was calcined at a temperature of 350ºC. The results show a somehow coherent outcome, giving very similar conversions. Then, it can also be observed that the conversion decreases about a 10% value, but only in the first 10-20 hours. After this, it keeps a quite constant value, indicating the catalyst was stable.

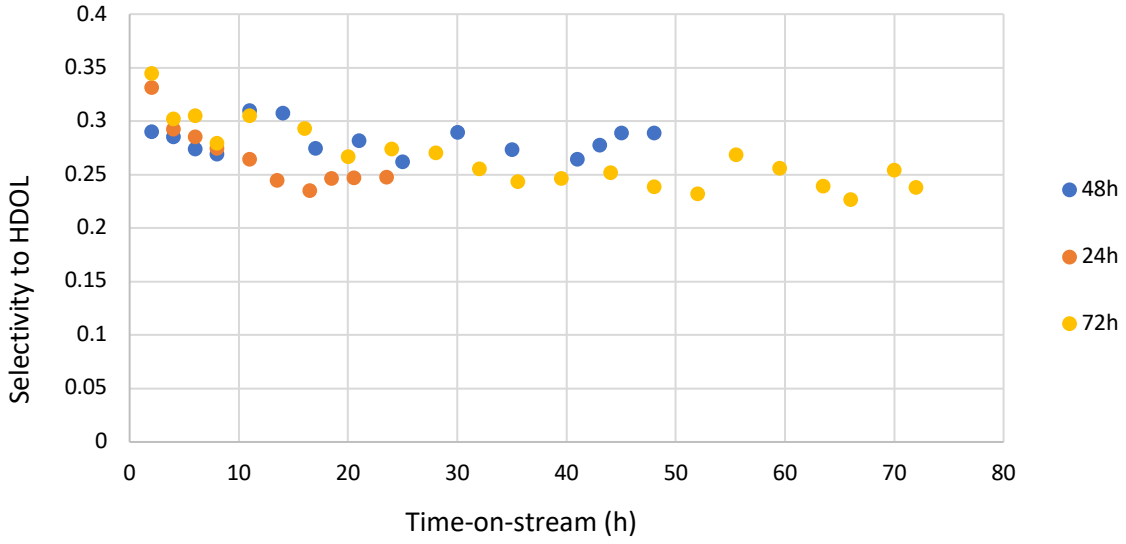

Figure 12. Selectivity towards HDOL over K18 catalyst.

Similarly to the Figure 11 results, in Figure 12 a linear trend is shown, where the selectivity does not vary dramatically and is mainly bounded between 25 and 30%.

After this first batch of test was performed, the catalyst was changed to the K19-350, as can be seen in Table 10, a 24h test was performed to verify its stability. Following this, a test performed with the catalyst being calcined at 550ºC, as stated in the catalyst characterization section, or a test with pauses of 1hour after each sample was taken and measured.

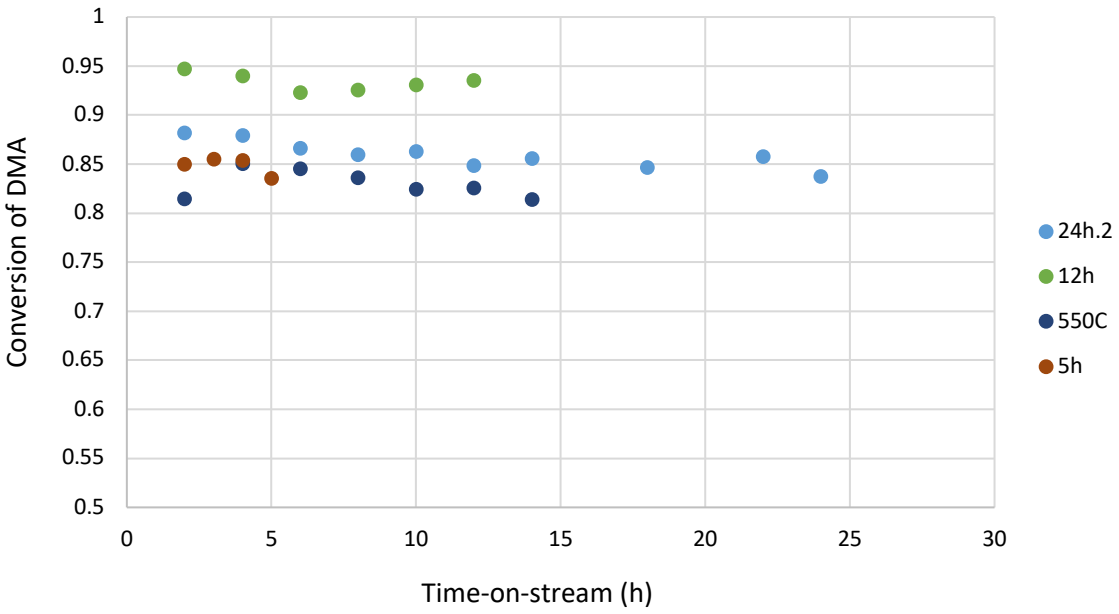

Figure 13. Conversion of DMA over K19 catalyst

These results can be observed in figure 13, where the conversion given by the k19 catalyst are plotted. We notice a slightly smaller conversion, and selectivity in figure 10, that could be explained by the results given by the BET analysis, that showed it had a smaller surface area in the catalyst, producing fewer places for the reaction to take place. The 24-hour test with the catalyst calcined at 350ºC gave very similar results to the K18 catalyst, but they show a 5-10% gain in conversion and a 10-15% gain in selectivity towards HDOL.

Finally, the best results were obtained in the 12-hour test with pauses of 1 hour after the samples were taken, giving an amazing 95% conversion over time without significant drops and outstanding 50% selectivity towards HDOL. However, this could be explained due to the fact that during this test, a small leak was detected and less DMA was flowing through the reactor, giving a higher conversion and selectivity.

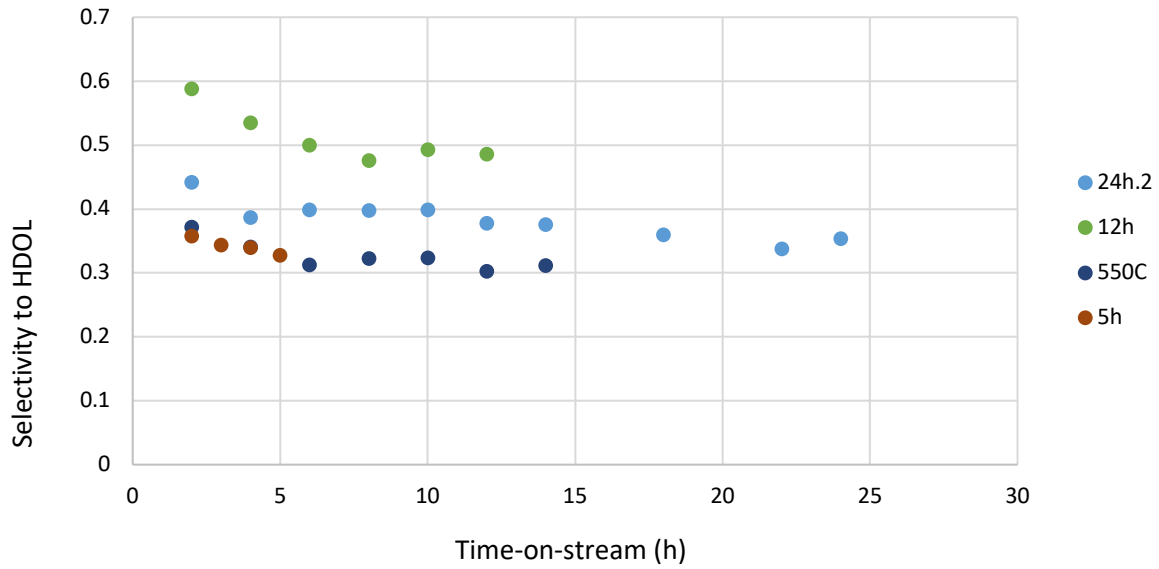

Figure 14. Selectivity to HDOL over K19 catalyst

Finally, in the next graph, named Figure 15, the relation between the selectivity and conversion can be seen. It is clear that there a linear trend, where when the conversion increases, the selectivity increases in a linear amount. It can be seen that the maximum theoretical selectivity would be 70% if the conversion was complete.

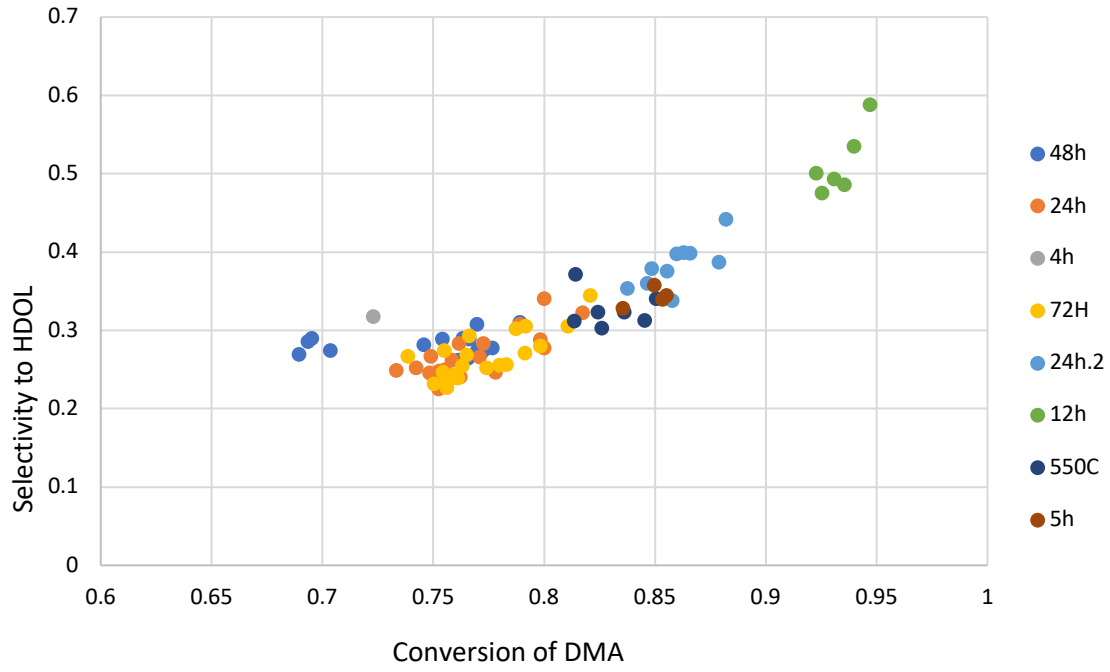

Figure 15. Relationship between selectivity and conversion.

Analyzing the results, it can be inferred that the k19 catalyst gives better performance in the hydrogenolysis of DMA towards HDOL. This can be due to several facts, but looking at the analysis done to the catalyst, some conclusions can be drawn. First, the higher concentration of zinc in the catalyst gives better performance due to preventing the copper particles from sintering and agglomerating. Also, with the higher zinc content catalyst, the 550 °C calcination temperature proved too high and gave worse selectivity and conversion rates. Moreover, the zincian malachite concentration in all as-prepared catalyst is very similar, but the presence of HTC crystalline phase could be the reason for a better outcome in the hydrogenolysis process.

When looking at the calcined catalyst, we see that the major crystalline phase in all of the catalyst samples is tenorite. However, in the better performing K19 catalyst, zincite can be detected, probably due to the higher zinc content. This could be thought as the needed phase for a higher selectivity, and in the future test, efforts should be made trying to increase its presence in the catalyst.

Gahnite could also be linked to the better performance of the k19_350 catalyst, since it is only seen in this sample, and this is the best performing one.

Finally, when looking at the K19 spent catalyst, the tenorite and cuprite concentration is still high, while in the K18 metallic copper is the main phase containing copper. Also, no aluminium compounds were detected, signaling that all of it was in the amorphous $(Cu,Zn)Al_XO_Y(CO_3)_Z$ structure.

Also, it is has been proved in Table 11 and 12, and the catalytic data, when the copper particles had a size in the 60-80 Å range, the best results were obtained, signaling this could be the sweet spot for the process trying to perform in these test.

CONCLUSIONS

In the branch of Green Chemistry, there has been the need to find a chromium free catalyst for ester hydrogenolysis. For this reason, the purpose of the project was to analyze the stability of a CuZnAl catalysts that have been pointed out as an appropriate substitute to the Adkins catalyst. During the tests, that ranged from 4 to 72h, a mean 75% conversion and 40% selectivity towards HDOL were obtained, with no significant drops being observed. Also, looking at the BET surface area, there was around a 20% decrease in BET surface area, but the drop seemed stable at all reaction times. For this, it can be concluded that the CuZnAl catalyst is a stable during tested time.

REFERENCES

(1) Anastas, P.; Eghbali, N. Green Chemistry: Principles and Practice. *Chem. Soc. Rev.* **2010**, *39* (1), 301–312. https://doi.org/10.1039/b918763b.

(2) R. A. Sheldon, Isabella Arends, U. H. *Green Chemistry and Catalysis*; WILEY-VCH, 2007.

(3) R. Rao, A. Dandekar, R. T. K. Baker, 1 and M. A. Vannice. Properties of Copper Chromite Catalysts in Hydrogenation Reactions. *J. Catal.* **1997**, No. CA971832, 406–419. https://doi.org/10.2514/6.1999-2319.

(4) Zhu, Y.; Zhu, Y.; Ding, G.; Zhu, S.; Zheng, H.; Li, Y. Highly Selective Synthesis of Ethylene Glycol and Ethanol via Hydrogenation of Dimethyl Oxalate on Cu Catalysts: Influence of Support. *Appl. Catal. A Gen.* **2013**, *468*, 296–304. https://doi.org/10.1016/j.apcata.2013.09.019.

(5) Prasad, R.; Singh, P. Applications and Preparation Methods of Copper Chromite Catalysts: A Review. *Bull. Chem. React. Eng. Catal.* **2011**, *6* (2), 63–114. https://doi.org/10.9767/bcrec.6.2.829.63-113.

(6) Nomura, K.; Ogura, H.; Imanishi, Y. K. Nomura Journal of Molecular Catalysis A Chemical, 2002, 178, 105–114..Pdf. **2002**, *178*, 105–114.

(7) Yuan, P.; Liu, Z.; Hu, T.; Sun, H.; Liu, S. Highly Efficient Cu-Zn-Al Catalyst for the Hydrogenation of Dimethyl Adipate to 1,6-Hexanediol: Influence of Calcination Temperature. *React. Kinet. Mech. Catal.* **2010**, *100* (2), 427–439. https://doi.org/10.1007/s11144-010-0190-2.

(8) Brands, D. S.; Poels, E. K.; Bliek, A. Ester Hydrogenolysis over Promoted Cu/SiO2catalysts. *Appl. Catal. A Gen.* **1999**, *184* (2), 279–289. https://doi.org/10.1016/S0926-860X(99)00106-4.

(9) Alexander, B. H. The Mechanism of Sintering of Copper. *Changes* **1967**.

(10) Ye, R. P.; Lin, L.; Li, Q.; Zhou, Z.; Wang, T.; Russell, C. K.; Adidharma, H.; Xu, Z.; Yao, Y. G.; Fan, M. Recent Progress in Improving the Stability of Copper-Based Catalysts for Hydrogenation of Carbon-Oxygen Bonds. *Catal. Sci. Technol.* **2018**, *8* (14), 3428–3449. https://doi.org/10.1039/c8cy00608c.

(11) Yuan, P.; Liu, Z.; Zhang, W.; Sun, H.; Liu, S. Cu-Zn/Al2O3 Catalyst for the Hydrogenation of Esters to Alcohols. *Cuihua Xuebao/Chinese J. Catal.* **2010**, *31* (7), 769–775. https://doi.org/10.1016/S1872-2067(09)60087-5.

(12) Figueiredo, R. T.; Martínez-Arias, A.; Granados, M. L.; Fierro, J. L. G. Spectroscopic Evidence of Cu–Al Interactions in Cu–Zn–Al Mixed Oxide Catalysts Used in CO Hydrogenation. *J. Catal.* **2002**, *178* (1), 146–152. https://doi.org/10.1006/jcat.1998.2106.

(13) Montassier, C.; Ménézo, J. C.; Moukolo, J.; Naja, J.; Hoang, L. C.; Barbier, J.; Boitiaux, J. P. Polyol Conversions into Furanic Derivatives on Bimetallic Catalysts: CuRu, CuPt and RuCu. *J. Mol. Catal.* **1991**, *70* (1), 65–84. https://doi.org/10.1016/0304-5102(91)85006-N.

(14) Gómez-Sainero, L.; Nocchetti, M.; Costantino, U.; Murcia-Mascarós, S.; Fierro, J. L. .; Navarro, R. . Oxidative Methanol Reforming Reactions on CuZnAl Catalysts Derived from Hydrotalcite-like Precursors. *J. Catal.* **2002**, *198* (2), 338–347. https://doi.org/10.1006/jcat.2000.3140.

(15) Semelsberger, T. A.; Ott, K. C.; Borup, R. L.; Greene, H. L. Generating Hydrogen-Rich Fuel-Cell Feeds from Dimethyl Ether (DME) Using Physical Mixtures of a Commercial Cu/Zn/Al2O3 Catalyst and Several Solid-Acid Catalysts. *Appl. Catal. B Environ.* **2006**, *65* (3–4), 291–300. https://doi.org/10.1016/j.apcatb.2006.02.015.

(16) Liu, C. B.; Qian, Z. Y.; Gu, Y. C.; Fan, L. Y.; Li, J.; Chao, G. T.; Jia, W. J.; Tu, M. J. Synthesis, Characterization, and Thermal Properties of Biodegradable Aliphatic Copolyester Based on ε-Caprolactone, Adipic Acid, and 1,6-Hexanediol. *Mater. Lett.* **2006**, *60* (1), 31–38. https://doi.org/10.1016/j.matlet.2005.07.074.

(17) Toba, M.; Tanaka, S. I.; Niwa, S. I.; Mizukami, F.; Koppány, Z.; Guczi, L.; Cheah, K. Y.; Tang, T. S. Synthesis

of Alcohols and Diols by Hydrogenation of Carboxylic Acids and Esters over Ru-Sn-Al2O3catalysts. *Appl. Catal. A Gen.* **1999**, *189* (2), 243–250. https://doi.org/10.1016/S0926-860X(99)00281-1.

(18) Šimáček, P.; Pospelova, V.; Tomášek, J.; Kikhtyanin, O.; Kubička, D.; Aubrecht, J. On the Importance of Transesterification By-Products during Hydrogenolysis of Dimethyl Adipate to Hexanediol. *Catal. Commun.* **2018**, *111* (January), 16–20. https://doi.org/10.1016/j.catcom.2018.03.006.

(19) Dos Santos, S. M.; Silva, A. M.; Jordão, E.; Fraga, M. A. Performance of RuSn Catalysts Supported on Different Oxides in the Selective Hydrogenation of Dimethyl Adipate. *Catal. Today* **2005**, *107–108*, 250–257. https://doi.org/10.1016/j.cattod.2005.07.076.

(20) Santos, S. M.; Silva, A. M.; Jordão, E.; Fraga, M. A. Hydrogenation of Dimethyl Adipate over Bimetallic Catalysts. *Catal. Commun.* **2004**, *5* (7), 377–381. https://doi.org/10.1016/j.catcom.2004.05.002.

(21) Figueiredo, F. C. A.; Jordão, E.; Carvalho, W. A. Dimethyl Adipate Hydrogenation at Presence of Pt Based Catalysts. *Catal. Today* **2005**, *107–108*, 223–229. https://doi.org/10.1016/j.cattod.2005.07.113.

(22) Silva, A. M.; Morales, M. A.; Baggio-Saitovitch, E. M.; Jordão, E.; Fraga, M. A. Selective Hydrogenation of Dimethyl Adipate on Titania-Supported RuSn Catalysts. *Appl. Catal. A Gen.* **2009**, *353* (1), 101–106. https://doi.org/10.1016/j.apcata.2008.10.025.

(23) Huang, Y.; Ariga, H.; Zheng, X.; Duan, X.; Takakusagi, S.; Asakura, K.; Yuan, Y. Silver-Modulated SiO2-Supported Copper Catalysts for Selective Hydrogenation of Dimethyl Oxalate to Ethylene Glycol. *J. Catal.* **2013**, *307*, 74–83. https://doi.org/10.1016/j.jcat.2013.07.006.

(24) Dai, W.-L.; Fan, K.; Wen, C.; Li, F.; Cui, Y. Investigation of the Structural Evolution and Catalytic Performance of the CuZnAl Catalysts in the Hydrogenation of Dimethyl Oxalate to Ethylene Glycol. *Catal. Today* **2013**, *233*, 117–126. https://doi.org/10.1016/j.cattod.2013.10.075.

(25) Yin, A.; Dai, W.-L.; Cui, Y.; Wen, C.; Fan, K. Remarkable Improvement of Catalytic Performance for a New Cobalt-Decorated Cu/HMS Catalyst in the Hydrogenation of Dimethyloxalate. *ChemCatChem* **2012**, *5* (1), 138–141. https://doi.org/10.1002/cctc.201200444.

(26) Dai, C. Z. D. W. P. M. Z. P. F. Y. P. Bin. Effect of Pd Doping on the Cu0/Cu+ Ratio of Cu-Pd/SiO2 Catalysts for Ethylene Glycol Synthesis from Dimethyl Oxalate. *Chem. Sel.* **2016**, *1* (11), 2857–2863.

(27) Wen, C.; Yin, A.; Cui, Y.; Yang, X.; Dai, W. L.; Fan, K. Enhanced Catalytic Performance for SiO2-TiO2 Binary Oxide Supported Cu-Based Catalyst in the Hydrogenation of Dimethyloxalate. *Appl. Catal. A Gen.* **2013**, *458*, 82–89. https://doi.org/10.1016/j.apcata.2013.03.021.

(28) Haber, J.; Block, J. .; Delmon, B. INTERNATIONAL UNION OF PURE MANUAL OF METHODS AND PROCEDURES FOR Manual of Methods and Procedures for Catalyst Characterization (Technical Report). *Pure Appl. Chem.* **1995**, *67*, 1257–1306.

(29) Girgsdies, F.; Nasrudin, N.; Hamid, S. B. A.; Kißner, S.; Brennecke, D.; Schlögl, R.; Muhler, M.; Kniep, B.; Busser, W.; Trunschke, A.; et al. Understanding the Complexity of a Catalyst Synthesis: Co-Precipitation of Mixed Cu,Zn,Al Hydroxycarbonate Precursors for Cu/ZnO/Al2O3 Catalysts Investigated by Titration Experiments. *Appl. Catal. A Gen.* **2010**, *392* (1–2), 93–102. https://doi.org/10.1016/j.apcata.2010.10.031.

(30) Osaki-T, V.-S. S.-K. Selective Production of Hydrogen by Partial Oxidation of Methanol over Catalysts Derived from CuZnAl-Layered Double Hydroxides. *Catalysis-Letters.* **1999**, *62 (2-4)* (340), 159–167.

(31) Behrens, M. Coprecipitation: An Excellent Tool for the Synthesis of Supported Metal Catalysts - From the Understanding of the Well Known Recipes to New Materials. *Catal. Today* **2015**, *246*, 46–54. https://doi.org/10.1016/j.cattod.2014.07.050.

(32) Fu, W.; Bao, Z.; Ding, W.; Chou, K.; Li, Q. The Synergistic Effect of the Structural Precursors of Cu/ZnO/Al 2O3 Catalysts for Water-Gas Shift Reaction. *Catal. Commun.* **2011**, *12* (6), 505–509. https://doi.org/10.1016/j.catcom.2010.11.017.

(33) Jeong, C.; Park, J.; Kim, J.; Baik, J. H.; Suh, Y. W. Effects of Al3+ Precipitation onto Primitive Amorphous Cu-Zn Precipitate on Methanol Synthesis over Cu/ZnO/Al2O3 Catalyst. *Korean J. Chem. Eng.* **2019**, *36* (2), 191–196. https://doi.org/10.1007/s11814-018-0186-6.

(34) Spencer, M. S. Precursors of Copper / Zinc Oxide Catalysts. **2000**, *66*, 255–257.